Phase transition in a rechargeable lithium battery

W. DREYER[1], M. GABERŠČEK[2], C. GUHLKE[1],

R. HUTH[1] and J. JAMNIK [2]

[1] *Weierstrass-Institute for Applied Analysis and Stochastics*

Mohrenstr. 39 10117 Berlin Germany

[2] *Kemijski Inštitut Ljubljana Slovenija*

L10 Laboratory for Materials Electrochemistry, SI-1001 Ljubljana Hajdrihova 19 Slovenija

(*Received 11 December 2009*)

We discuss the lithium storage process within a single particle cathode of a lithium-ion battery. The single storage particle consists of a crystal lattice whose interstitial lattice sites may be empty or reversibly filled with lithium atoms. The resulting evolution equations describe diffusion with mechanical coupling and incorporate volume changes, phase transitions and surface tension.

In order to simulate the dynamics we assume spherical symmetry and fast bulk diffusion of the lithium atoms, which leads to a core shell model. We verify the common assumption of phase nucleation at the external boundary of the particle.

This model is capable to predict voltage capacity behavior. For slow charging rates, we compare the results with experimental voltage capacity plots exhibiting hysteretic

behavior. We observe that hysteresis cannot be described within the setting of a single particle cathode. The origin of this fact is discussed in detail.

The result is of enormous importance because single particle models, in particular core shell models, up to now are very popular in the chemical literature.

1 Introduction

The arrangement shown in Figure 1 roughly indicates the processes in a lithium battery during discharging and charging. During discharging electrons leave the anode to travel through an outer circuit. The anode is here assumed to be a metallic lithium electrode. The remaining positive lithium ions leave the anode and move through an electrolyte towards the cathode, which is the central object of the current modelling. We consider a modern cathode that consists of a carbon coated single crystal $FePO_4$ with the shape of a small sphere of about 20 nm diameter. The $FePO_4$ lattice offers interstitial lattice sites that serve to store lithium atoms. When the battery is fully charged, all interstitial lattice sites are empty. During discharging the arriving lithium ions combine at the carbon coated surface of the $FePO_4$ ball with the inflowing electrons and hereafter they occupy the interstitial lattice sites. After complete discharging a maximal number of sites of the interstitial lattice is occupied by a lithium atom. During recharging of the battery the reverse process takes place.

The objective of the current study is the modelling of the loading/unloading processes of the $FePO_4$ lattice with lithium atoms. The model describes diffusion with mechanical coupling within an open system. It relies on various experimental observations and assumptions:

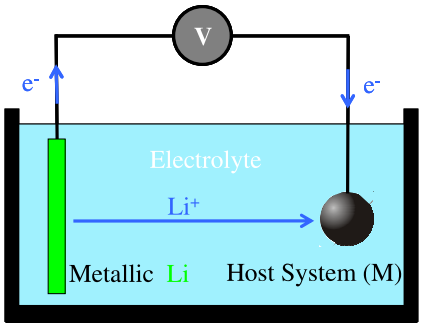

FIGURE 1. Basic constituents of a rechargeable lithium battery

1. The voltage - charge plot, see Figure 2 exhibits a hysteretic behavior. The characteristics of voltage against the total charge of the battery during charging, blue arrows, is different from discharging, red arrows.

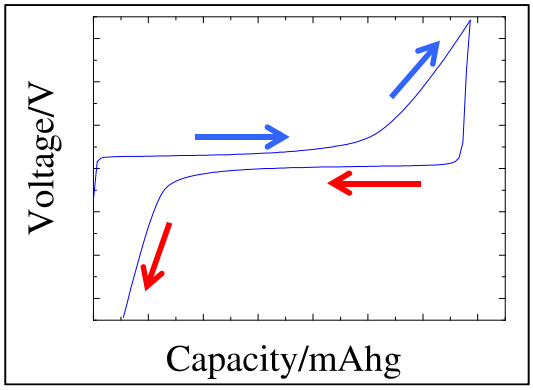

FIGURE 2. Typical charge and discharge curve for a $LiFePO_4$ cathode. The voltage is plotted as a function of the total charge per mass. The charging (blue arrows) and discharging (red arrows) were performed under constant current regime. The electrode was prepared as described by Gaberščck et al. [9].

2. The lithium atoms need more space as is offered by the interstitial lattice sites. In case of a fixed external pressure, this leads to a change of the volume of the $FePO_4$ ball up to 6% for the fully occupied interstitial lattice.

3. There is a compact region of total lithium fraction where the distribution of the lithium atoms within the $FePO_4$ ball decomposes into two phases with different lithium mole fractions across the interface between the adjacent phases. Currently we assume that there is a single interface with the shape of a sphere. Thus in the 2-phase region we currently deal with an inner core and an outer shell. Furthermore we assume that the interface originates at the outer surface during loading as well as during unloading.

4. At the interface of the two phases we take surface tension into account, which is of importance due to the small interfacial radius.

Finally we mention a recent study, see [15], by Wagemaker, Borghols and Mulder. The authors observe a strong dependence between the maximal possible Li content and the size of the host system, and they conjecture likewise mechanical effects as the origin for this phenomenon. In fact, it is a typical feature of the mechanical boundary value problem, that the size of the considered system is of large influence.

We have organized the paper as follows:

In Chapter 2 we describe the constitution of the host system. The thermodynamic model is developed in Chapter 3. This model relies on local conservation laws in the bulk phases, on jump conditions, i.e. Stefan conditions, across the interface and in particular on so called kinetic relations, which relates the interfacial motion to the corresponding driving force. We end up with a system of nonlinear diffusion equations with mechanical coupling.

Chapter 4 considers the limiting case of infinite bulk mobility, whereby we may reduce the PDE system into an ODE system for the Li mole fraction, the interfacial radius and the external radius of the $FePO_4$ ball as functions of time.

This ODE is analysed in Chapter 5. We determine the possible equilibria and examine the evolution of the host system for slow charging rate.

2 Constitution of the host system

The mechanical constitution of the host system from Figure 1 is described in detail by T. Maxisch and G. Ceder in [12]. It is composed of a deformable crystal lattice of the substance $FePO_4$. The undeformed crystal has orthorhombic olivine symmetry. Furthermore there is a sublattice whose lattice sites may be empty or occupied by Li atoms. These can be supplied or removed through the external boundary, and this process is called *lithiation*. To each unit of $FePO_4$ there corresponds one single site in the sublattice. The occupation of the sublattice with Li atoms does not change the orthorhombic olivine symmetry. However, the elastic stiffness coefficients and the crystal volume change if the number of Li atoms is changed.

At room temperature there exists a region of total Li mole fraction where the distribution of Li atoms on the sublattice sites is realized by two coexisting phases that differ by high and small Li mole fraction. Theoretical studies on the evolution of Li atoms in the host system by Han et al. [11], Srinivasan and Newman [14] and the current study rely on this phenomenon, which is experimentally investigated by Yamada et al. [16].

Based on previous studies by Srinivasan and Newman [14] and Han et al. [11], we currently also assume that the two phases exhibit a simple morphology: They appear as an inner spherical core and an outer shell with a moving interface. However, it is important to note that in 2007 this assumed symmetry is criticized by Allen, Jow and

Wolfenstine [1]. Due to some experimental hints these authors prefer a plane interface that may move in some preferred direction of the matrix lattice.

3 Thermodynamic description of the host system

3.1 Conservation laws of particle numbers

We consider the host system as a body Ω that may be represented by a single phase or by two coexisting phases, so that $\Omega = \Omega_- \cup \Omega_+$ as indicated in Figure 3. The inner core is denoted Ω_- with radius $r_{\rm I}$, respectively Ω_+ denotes the outer shell with radius r_0. At any time $t \geq 0$, the thermodynamic state of the body Ω is described by a certain number of variables, which may be functions of space $x = (x^i)_{i=1,2,3} = (x^1, x^2, x^3) \in \Omega$. The host system consists of three constituents: There are $FePO_4$ units (M) generating

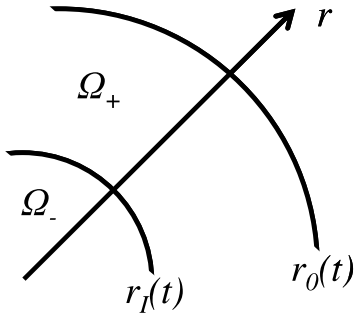

FIGURE 3. The 2-phase morphology of the host system

the deformable lattice, which we shall call the matrix lattice. The matrix lattice has orthorhombic symmetry in the undeformed state. Furthermore there is an interstitial sublattice, whose constituents are Li atoms (Li) and vacancies (V). The number densities of the constituents are denoted by $n_{\rm M}$, $n_{\rm Li}$ and $n_{\rm V}$.

Among the objectives of this study is the determination of the functions

$$n_{\mathrm{M}}(t,x), \quad n_{\mathrm{Li}}(t,x), \quad n_{\mathrm{V}}(t,x) \quad \text{and} \quad r_{\mathrm{I}}(t), \quad r_0(t). \tag{3.1}$$

We assume that there is no diffusion on the matrix lattice, which is fully occupied by the $FePO_4$ units, so that $n_{\mathrm{M}}(t,x)$ changes exclusively due to the deformation of the lattice. On the sublattice we have diffusion, which, however, is restricted by the side condition that matrix lattice and sublattice have equal number of lattice sites, thus we have

$$n_{\mathrm{M}}(t,x) = n_{\mathrm{Li}}(t,x) + n_{\mathrm{V}}(t,x). \tag{3.2}$$

Next we introduce the velocities $\upsilon = (\upsilon^i)_{i=1,2,3} = (\upsilon^1, \upsilon^2, \upsilon^3)$ of the constituents by the functions

$$\upsilon_{\mathrm{M}}(t,x), \qquad \upsilon_{\mathrm{Li}}(t,x), \qquad \upsilon_{\mathrm{V}}(t,x) \tag{3.3}$$

The conservation laws for the particle numbers then read in Ω_- and Ω_+

$$\begin{aligned} \frac{\partial n_{\mathrm{M}}}{\partial t} + \operatorname{div}(n_{\mathrm{M}}\upsilon_{\mathrm{M}}) &= 0, \\ \frac{\partial n_{\mathrm{Li}}}{\partial t} + \operatorname{div}(n_{\mathrm{Li}}\upsilon_{\mathrm{Li}}) &= 0, \\ \frac{\partial n_{\mathrm{V}}}{\partial t} + \operatorname{div}(n_{\mathrm{V}}\upsilon_{\mathrm{V}}) &= 0. \end{aligned} \tag{3.4}$$

The constraint (3.2) and the conservation laws (3.4) motivate the following property for the matrix velocity υ_{M}

$$n_{\mathrm{M}}\upsilon_{\mathrm{M}}(t,x) = n_{\mathrm{Li}}\upsilon_{\mathrm{Li}}(t,x) + n_{\mathrm{V}}\upsilon_{\mathrm{V}}(t,x). \tag{3.5}$$

Due to (3.2) and (3.5) there are only two independent conservation laws.

If the state of the host system is in the 2-phase region, singular points will appear at the interface I between the adjacent phases. At I the conservation laws of particle

numbers assume the form

$$\begin{aligned} -w^\nu[[n_{\mathrm{M}}]] + [[n_{\mathrm{M}} v_{\mathrm{M}}^\nu]] &= 0, \\ -w^\nu[[n_{\mathrm{Li}}]] + [[n_{\mathrm{Li}} v_{\mathrm{Li}}^\nu]] &= 0, \\ -w^\nu[[n_{\mathrm{V}}]] + [[n_{\mathrm{V}} v_{\mathrm{V}}^\nu]] &= 0. \end{aligned} \tag{3.6}$$

Herein $w^\nu = w \cdot \nu$ denotes the normal speed of the interface ν is the normal vector, which points into the + region and $v^\nu = v \cdot \nu$ is the constituents velocity in normal direction. Double brackets denote the difference of a quantity that suffers a discontinuity at the interface: $[[\psi]] = \psi_+ - \psi_-$.

We conclude that the atomic fluxes

$$\begin{aligned} \dot{\mathcal{N}}_{\mathrm{M}} &\equiv -n_{\mathrm{M}}(v_{\mathrm{M}}^\nu - w^\nu), \\ \dot{\mathcal{N}}_{\mathrm{Li}} &\equiv -n_{\mathrm{Li}}(v_{\mathrm{Li}}^\nu - w^\nu) \quad \text{and} \\ \dot{\mathcal{N}}_{V} &\equiv -n_{\mathrm{V}}(v_{\mathrm{V}}^\nu - w^\nu) \end{aligned} \tag{3.7}$$

are continuous across the interface, i.e.

$$\dot{\mathcal{N}}_{\mathrm{M}}^+ = \dot{\mathcal{N}}_{\mathrm{M}}^-, \quad \dot{\mathcal{N}}_{\mathrm{Li}}^+ = \dot{\mathcal{N}}_{\mathrm{Li}}^-, \quad \text{and} \quad \dot{\mathcal{N}}_{\mathrm{V}}^+ = \dot{\mathcal{N}}_{\mathrm{V}}^-. \tag{3.8}$$

In the considered case of spherical morphology, the interface is completely described by its time dependent radius $r_{\mathrm{I}}(t)$. In this case we have in polar coordinates $\nu = (1, 0, 0)$ and $w^\nu = \dot{r}_{\mathrm{I}}(t)$. Likewise as in the bulk, only two conservation laws of (3.7) are independent.

The quantities that appear in the conservation laws of particle numbers can be combined to define further quantities that are needed for the description of the thermodynamic state of the host system. Among these are the mass density ρ and the barycentric velocity v, which are defined by

$$\rho \equiv m_{\mathrm{Li}} n_{\mathrm{Li}} + m_{\mathrm{M}} n_{\mathrm{M}} \qquad \text{and} \qquad \rho v \equiv m_{\mathrm{Li}} n_{\mathrm{Li}} v_{\mathrm{Li}} + m_{\mathrm{M}} n_{\mathrm{M}} v_{\mathrm{M}}, \tag{3.9}$$

where m_{M} and m_{Li} denote the atomic masses of $FePO_4$ and Li. Note that the vacancies do not contribute to mass density and barycentric velocity .

A linear combination of the conservation laws for the particle numbers imply the conservation laws for the total mass, viz.

$$\begin{aligned} \frac{\partial \rho}{\partial t} + \operatorname{div}(\rho \upsilon) = 0 \quad \text{for} \quad x \in \Omega_{+/-} \quad \text{and} \\ -w^{\nu}[[\rho]] + [[\rho \upsilon^{\nu}]] = 0 \quad \text{for} \quad x \in I. \end{aligned} \tag{3.10}$$

Next we introduce the atomic fraction of Li, y, and the diffusion fluxes with respect to the velocity υ_{M} of the crystal lattice, $j_{\mathrm{Li}} = (j^i_{\mathrm{Li}})_{i=1,2,3}$ and $j_{\mathrm{V}} = (j^i_{\mathrm{V}})_{i=1,2,3}$:

$$y \equiv \frac{n_{\mathrm{Li}}}{n_{\mathrm{M}}}, \quad j_{\mathrm{Li}} \equiv n_{\mathrm{Li}}(\upsilon_{\mathrm{Li}} - \upsilon_{\mathrm{M}}), \quad j_{\mathrm{V}} \equiv n_{\mathrm{V}}(\upsilon_{\mathrm{V}} - \upsilon_{\mathrm{M}}). \tag{3.11}$$

Diffusion fluxes with respect to the barycentric velocity υ are also important, $f_{\mathrm{Li}} = (f^i_{\mathrm{Li}})_{i=1,2,3}$, $f_{\mathrm{V}} = (f^i_{\mathrm{V}})_{i=1,2,3}$ and $f_{\mathrm{M}} = (f^i_{\mathrm{M}})_{i=1,2,3}$:

$$\begin{aligned} f_{\mathrm{Li}} &\equiv n_{\mathrm{Li}}(\upsilon_{\mathrm{Li}} - \upsilon), \\ f_{\mathrm{V}} &\equiv n_{\mathrm{V}}(\upsilon_{\mathrm{V}} - \upsilon) \quad \text{and} \\ f_{\mathrm{M}} &\equiv n_{\mathrm{M}}(\upsilon_{\mathrm{M}} - \upsilon). \end{aligned} \tag{3.12}$$

Finally we list several identities between the various diffusion fluxes. They read

$$\begin{aligned} j_{\mathrm{Li}} + j_{\mathrm{V}} = 0, \qquad m_{\mathrm{Li}} f_{\mathrm{Li}} + m_{\mathrm{M}} f_{\mathrm{M}} = 0, \\ f_{\mathrm{Li}} = j_{\mathrm{Li}} + y f_{\mathrm{M}}, \qquad f_{\mathrm{V}} = j_{\mathrm{V}} + (1-y) f_{\mathrm{M}}, \end{aligned} \tag{3.13}$$

and at the interface we have

$$m_{\mathrm{Li}} \dot{\mathcal{N}}_{\mathrm{Li}} + m_{\mathrm{M}} \dot{\mathcal{N}}_{\mathrm{M}} = -\rho(\upsilon^{\nu} - w^{\nu}). \tag{3.14}$$

3.2 Conservation law of momentum

The conservation law of momentum determines the motion of the matrix lattice, i.e. the displacement $u = (u^i)_{i=1,2,3} = (u^1, u^2, u^3)$. If we ignore elastic waves in the matrix lattice, this conservation law reduces to a quasi-static force balance, which reads in regular points in Ω

$$\operatorname{div} \sigma = 0. \tag{3.15}$$

The newly introduced quantity $\sigma = (\sigma^{ij})_{i,j=1,2,3}$ is the Cauchy stress tensor with $\sigma^{ij} = \sigma^{ji}$. Here we apply a simplified mechanical model that ignores (i) the orthorhombic symmetry and (ii) the deviatoric stresses so that the stress tensor reduces to a pressure p: $\sigma^{ij} = -p\delta^{ij}$.

The quasi-static momentum balance at the interface I is given by

$$[[\sigma^{ij}]]\nu^j = -2\gamma k_M \nu^i \tag{3.16}$$

and for the special case at hand

$$[[p]] = -\frac{2\gamma}{r_{\mathrm{I}}}. \tag{3.17}$$

$\gamma > 0$ is the surface tension and k_M denotes the mean curvature, which reads in polar coordinates for a sphere: $k_M = -1/r_{\mathrm{I}}$.

3.3 Constitutive Model, Part 1: Some pieces of the second law of thermodynamics

In this and the following sections we rely on the recent study by Dreyer et al. [4] to show that the knowledge of the free energy is sufficient in order to give all constitutive quantities as functions of the variables. Here we start with the assumption that the

specific free energy ψ, is given by the general representations

$$\psi = \hat{\psi}(T, n_{\mathrm{Li}}, n_{\mathrm{V}}) = \tilde{\psi}(T, y, \rho), \tag{3.18}$$

where T is the temperature, which is throughout this paper assumed to be constant. The functions $\hat{\psi}$ and $\tilde{\psi}$ are related to each other in a simple manner by means of the transformation

$$y = \frac{n_{\mathrm{Li}}}{n_{\mathrm{Li}} + n_{\mathrm{V}}} = \frac{n_{\mathrm{Li}}}{n_{\mathrm{M}}} \quad \text{and} \quad \rho = (n_{\mathrm{Li}} + n_{\mathrm{V}})m(y) = n_{\mathrm{M}} m(y) \tag{3.19}$$

with $m(y) \equiv m_{\mathrm{M}} + m_{\mathrm{Li}} y$. In the following, the function $\hat{\psi}$ will be used to calculate the chemical potentials μ_{Li} and μ_{V} whereas $\tilde{\psi}$ gives the pressure p. According to the 2$^{\mathrm{nd}}$ law of thermodynamics we have, see [4] for details,

$$\begin{aligned} \mu_{\mathrm{Li}} &= \frac{\partial \rho \hat{\psi}}{\partial n_{\mathrm{Li}}}, \qquad \mu_{\mathrm{V}} = \frac{\partial \rho \hat{\psi}}{\partial n_{\mathrm{V}}}, \\ p &= \rho^2 \frac{\partial \tilde{\psi}}{\partial \rho}, \qquad \rho\psi + p = \mu_{\mathrm{Li}} n_{\mathrm{Li}} + \mu_{\mathrm{V}} n_{\mathrm{V}}. \end{aligned} \tag{3.20}$$

The equations $(3.20)_1$ to $(3.20)_3$ give some parts of the Gibbs equation and $(3.20)_4$ is called Gibbs-Duhem equation. The explicit form of the functions $\hat{\psi}$ and $\tilde{\psi}$ will be given and exploited in the next section.

A further content of the 2$^{\mathrm{nd}}$ law of thermodynamics is the entropy inequality, which identifies on its left hand side the entropy production in the two bulk phases. It reads

$$-f_{\mathrm{Li}} \nabla \mu_{\mathrm{Li}} - f_{\mathrm{V}} \nabla \mu_{\mathrm{V}} = -f_{\mathrm{Li}} \nabla \Big(\mu_{\mathrm{Li}} - \frac{m_{\mathrm{Li}} + m_{\mathrm{M}}}{m_{\mathrm{M}}} \mu_{\mathrm{V}} \Big) \geq 0. \tag{3.21}$$

The equality sign holds in equilibrium, where the entropy production assumes its minimum value zero. In non-equilibrium the production of entropy must be positive. Thus in equilibrium we have $f_{\mathrm{Li}} = 0$ and $\nabla(\mu_{\mathrm{Li}} - (m_{\mathrm{Li}} + m_{\mathrm{M}})/m_{\mathrm{M}}\ \mu_{\mathrm{V}}) = 0$.

The most simple possibility to satisfy the entropy inequality in non-equilibrium is given

by Fick's law

$$f_{\mathrm{Li}} = -M^{\mathrm{B}}(T,y)\nabla\Big(\mu_{\mathrm{Li}} - \frac{m_{\mathrm{Li}}+m_{\mathrm{M}}}{m_{\mathrm{M}}}\mu_{\mathrm{V}}\Big), \tag{3.22}$$

where the bulk mobility satisfies $M^{\mathrm{B}}(T,y) > 0$.

Note that the entropy inequality holds point-wise, thus there is also an inequality at the interface I, viz.

$$-\rho(\upsilon^\nu - w^\nu)[[\psi + \frac{1}{2}(\upsilon - w)^2]] + [[\sigma^{ij}(\upsilon^i - w^i)]]\nu^j - [[\mu_{\mathrm{Li}} f^\nu_{\mathrm{Li}} + \mu_{\mathrm{V}} f^\nu_{\mathrm{V}}]] \geq 0. \tag{3.23}$$

The derivation of the entropy inequalities (3.21) and (3.23) can be found in [3] and [4]. In particular details concerning the treatment of vacancies and side conditions are given there.

The interfacial entropy production will be used to formulate relations that are similar to Fick's law in the bulk phases. To this end we bring the left hand side of (3.23) by means of $\sigma^{ij} = -p\delta^{ij}$, the flux definitions (3.11), (3.12) and (3.7), the conservation laws (3.8), the Gibbs-Duhem relation $(3.20)_4$ and the identities (3.13) and (3.14) into a more appropriate form:

$$\dot{\mathcal{N}}_{\mathrm{Li}}[[\mu_{\mathrm{Li}} - \mu_{\mathrm{V}} + \frac{m_{\mathrm{Li}}}{2}(\upsilon - w)^2]] + \dot{\mathcal{N}}_{\mathrm{M}}[[\mu_{\mathrm{V}} + \frac{m_{\mathrm{M}}}{2}(\upsilon - w)^2]] \geq 0. \tag{3.24}$$

Note the similarity between (3.21) and (3.24). In any case the entropy production is a sum of products *flux* $\times$ *driving force*. In (3.21) the flux is the diffusion flux of Li and the driving force has to be identified with the gradient of a chemical potential difference. At the interface two products contribute to the entropy production: The flux of the first contribution is the atomic Li flux across the interface and the jump of the chemical potential difference plus a kinetic contribution is the driving force. The flux of

the second product is identified as the atomic $FePO_4$ flux and the driving force is the jump consisting of the chemical potential of the vacancies plus a kinetic contribution. Both kinetic contributions are often small in comparison with the chemical potentials.

The equality sign of (3.24) holds in equilibrium and in non-equilibrium the interfacial entropy production must be positive. Thus in equilibrium we have $\dot{\mathcal{N}}_{\mathrm{Li}} = 0$ and $\dot{\mathcal{N}}_{\mathrm{M}} = 0$, and the possible equilibria are determined by

$$[[\mu_{\mathrm{Li}} - \mu_{\mathrm{V}}]] = 0 \quad \text{and} \quad [[\mu_{\mathrm{V}}]] = 0. \tag{3.25}$$

In an analogous manner to the bulk, the simplest possibility to satisfy the interfacial entropy production in equilibrium as well as in non-equilibrium is given by the ansatz

$$\begin{aligned} \dot{\mathcal{N}}_{\mathrm{Li}} &= M^{\mathrm{I}}_{Li}[[\mu_{\mathrm{Li}} - \mu_{\mathrm{V}} + \frac{m_{\mathrm{Li}}}{2}(v - w)^2]], \quad \text{and} \\ \dot{\mathcal{N}}_{\mathrm{M}} &= M^{\mathrm{I}}_{M}[[\mu_{\mathrm{V}} + \frac{m_{\mathrm{M}}}{2}(v - w)^2]]. \end{aligned} \tag{3.26}$$

Thus there are two positive mobilities at the interface, viz. M^{I}_{Li} and M^{I}_{M}.

We may conclude from the results of this section that if we were to know the free energy density, we could calculate all the other constitutive quantities. However, the bulk mobility and the two interfacial mobilities must be determined either by statistical thermodynamics or by experiments.

3.4 Constitutive law, Part2: Explicit forms of the pressure, free energy density and chemical potentials

The strategy to determine the specific free energy, i.e. the two functions $\hat{\psi}(T, n_{\mathrm{Li}}, n_{\mathrm{V}})$ and $\tilde{\psi}(T, y, \rho)$, is as follows: At first we use $(3.20)_3$ to determine the ρ dependence of the function $\tilde{\psi}$, which is given by the pressure. To this end we start with a constitutive law

that relates the pressure to the volume change of the matrix lattice. We assume

$$p = \bar{p} + K\Big(\frac{n_{\mathrm{M}}}{\bar{n}_{\mathrm{M}}} - h(y)\Big) \quad \text{with} \quad h(y) = \frac{1}{1+y\delta}\ . \tag{3.27}$$

The difference $n_{\mathrm{M}}/\bar{n}_{\mathrm{M}} - h(y)$ gives the volumetric strain of the $\mathrm{Li}_y\mathrm{FePO}_4$ matrix with respect to a strain $h(y)$ that describes the change of matrix volume due to a variation of the Li mole fraction at constant reference pressure $\bar{p}$. The quantity $\bar{n}_{\mathrm{M}}$ denotes the particle density of FePO_4 at the reference pressure and for $y = 0$. The bulk modulus is denoted by K. According to [12], K depends on the Li fraction y, but we ignore that fact here. The function $h(y)$ describes the phenomenon that Li atoms need more space than the vacancies. If $\delta = 0$ we were to have $n_{\mathrm{M}} = \bar{n}_{\mathrm{M}}$ at $p = \bar{p}$. However, there is a volumetric expansion $(V - \bar{V})/\bar{V}$ of the host system if the Li fraction changes from 0 to 1. We denote its maximum for $y = 1$ by $\delta \equiv (V_{\max} - \bar{V})/\bar{V}$, which is about 0.06. For other values of y we simply interpolate and write $(V - \bar{V})/\bar{V} = y\delta$. The volume expansion is measured at the reference pressure, where we have $n_{\mathrm{M}}/\bar{n}_{\mathrm{M}} = h(y)$, on the other hand $n_{\mathrm{M}}/\bar{n}_{\mathrm{M}} = \bar{V}/V$, therefore we obtain $h(y)$ as it is given by $(3.27)_2$.

Next we apply $(3.20)_3$ to calculate the mechanical part of the free energy from the pressure. Since the derivative of the function $\tilde{\psi}$ depends on the variables T, y and ρ, we represent p in the same variables, and we integrate

$$\frac{\partial\tilde{\psi}}{\partial\rho} = \frac{p}{\rho^2} = \frac{\bar{p} - Kh(y)}{\rho^2} + \frac{K}{\bar{n}_{\mathrm{M}} m(y)}\frac{1}{\rho}. \tag{3.28}$$

We obtain

$$\begin{aligned}\rho\tilde{\psi}(T,y,\rho) = (\bar{p} - Kh(y))\Big(\frac{\rho}{\bar{n}_{\mathrm{M}} m(y) h(y)} - 1\Big) + \\ + K\frac{\rho}{\bar{n}_{\mathrm{M}} m(y)} \log\Big(\frac{\rho}{\bar{n}_{\mathrm{M}} m(y) h(y)}\Big) + \rho C(T,y).\end{aligned} \tag{3.29}$$

We have chosen the integration constant so that the remaining unknown function $C(T, y)$

can be identified with the chemical part of the free energy density: $\tilde{\psi}^{\mathrm{chem}}(T,y) \equiv C(T,y)$. In this context, the mechanical part of the free energy density is defined by $\rho\psi^{\mathrm{mech}} \equiv \rho\psi - \rho\psi^{\mathrm{chem}}$.

The motivation of that decomposition relies on the fact, that our knowledge on the two contributions to the free energy originates from different sources. The chemical part can be calculated within statistical thermodynamics. The simplest model that is capable to exhibit two coexisting phases is given by,

$$\rho\psi^{\mathrm{chem}} = n_{\mathrm{M}}\Omega\left(y(1-y) + \frac{kT}{\Omega}\Big(y\log(y) + (1-y)\log(1-y)\Big)\right) \equiv n_{\mathrm{M}}\Omega f(y)\ . \quad (3.30)$$

Here k denotes the Boltzmann constant. We omit the argument T in f since we explicitly assume T to be constant. The first term gives an energetic contribution whose strength is controlled by the constant $\Omega > 0$, whereas the second contribution is purely entropic. Note that the positivity of Ω may lead to a non-convex function, which is necessary to obtain two coexisting phases. The phase field approach by Han et al. [11] uses the same function $f(y)$.

Next we calculate the chemical potentials according to $(3.20)_1$ and $(3.20)_2$. For this we need the identities derived from (3.2), (3.19) and $n_{\mathrm{M}} = \hat{n}_{\mathrm{M}}(n_{\mathrm{Li}}, n_{\mathrm{V}})$, $y = \hat{y}(n_{\mathrm{Li}}, n_{\mathrm{V}})$,

$$\frac{\partial n_{\mathrm{M}}}{\partial n_{\mathrm{Li}}} = 1, \quad \frac{\partial n_{\mathrm{M}}}{\partial n_{\mathrm{V}}} = 1, \quad \frac{\partial y}{\partial n_{\mathrm{Li}}} = \frac{1-y}{n_{\mathrm{M}}}, \quad \frac{\partial y}{\partial n_{\mathrm{V}}} = -\frac{y}{n_{\mathrm{M}}}\ . \quad (3.31)$$

We obtain for Li

$$\begin{aligned}\frac{1}{\Omega}\mu_{\mathrm{Li}} &= f + (1-y)f' \\ &\quad + a_1\left(\log\Big(\frac{n_{\mathrm{M}}}{\bar{n}_{\mathrm{M}}h}\Big) - \frac{h'}{h}\Big(1 - \frac{\bar{n}_{\mathrm{M}}h}{n_{\mathrm{M}}}\Big)(1-y)\right) + a_2\left(1 - \frac{h'}{h}(1-y)\right)\frac{1}{h},\end{aligned} \quad (3.32)$$

and for the vacancies

$$\begin{aligned}\frac{1}{\Omega}\mu_{\mathrm{V}} &= f - yf' \\ &\quad + a_1\left(\log\left(\frac{n_{\mathrm{M}}}{\bar{n}_{\mathrm{M}}h}\right) + \frac{h'}{h}\Big(1-\frac{\bar{n}_{\mathrm{M}}h}{n_{\mathrm{M}}}\Big)y\right) + a_2\left(1+\frac{h'}{h}y\right)\frac{1}{h}.\end{aligned} \tag{3.33}$$

The newly introduced constants $a_1 = K/\bar{n}_{\mathrm{M}}\Omega$ and $a_2 = \bar{p}/\bar{n}_{\mathrm{M}}\Omega$ control the strength of mechanical in comparison to chemical driving forces.

4 The model for infinite bulk diffusivity and spherical symmetry

In this section we exploit the thermodynamic model for the host system under some assumptions that will drastically simplify the analysis. The general case will be treated in a forthcoming study.

4.1 Simplifying assumptions

Recall that the model contains three inherent time scales, and a fourth time scale is given by the boundary conditions. These scales can be extracted from the mobility in the bulk, M^{B}, the mobilities for interfacial kinetics, $M^{\mathrm{I}}_{\mathrm{Li}}$ and $M^{\mathrm{I}}_{\mathrm{M}}$, and the speed of supply and removal of Li atoms at the outer boundary. Relying on data found in [11], we now assume that the fastest of these processes is diffusion in the bulk, and we consider the limiting case of infinite bulk mobility. In other words: For finite diffusion flux and infinite bulk mobility, the chemical potentials and thus the number densities of the constituents become homogeneous within the two phases, because Fick's law (3.22), viz. $f_{\mathrm{Li}} = -M^{\mathrm{B}}\nabla(\mu_{\mathrm{Li}} - (m_{\mathrm{Li}} + m_{\mathrm{M}})/m_{\mathrm{M}}\ \mu_{\mathrm{V}})$, assumes the form $f_{\mathrm{Li}} = -\infty \times 0$ and thus cannot be used anymore to determine the diffusion flux in this limiting case. In fact we

shall see that for infinite bulk mobility f_{Li} follows from the local conservation law for the Li content.

In Section 3.4 we have already ignored the orthorhombic symmetry of the matrix lattice and the deviatoric stress components, so that the constitutive law (3.27) for the pressure is sufficient to describe the deformation of the lattice.

A further assumption concerns the geometric shape of the host system and of the interface I. We assume that the host system is a sphere with outer time dependent radius $r_0(t)$, and the morphology of the distribution of the two phases is an inner core Ω_- with interfacial radius $r_{\mathrm{I}}(t)$ and an outer shell Ω_+. It is important to note that this assumption has been criticized by Allen et al., see [1].

Finally we have to fix the location $r_{\mathrm{I}}(t_0)$ where the interface starts when we enter into the 2-phase region. Loading and unloading of the host system with Li atoms happens at the outer boundary. Despite the idealized assumption of homogeneity of the densities in bulk, it is obvious that if we reach the 2-phase region by supply of Li at r_0, the Li fraction will be slightly larger here than in the interior, so that the interface will start at the outer boundary for the loading process. On the other hand, the interface will also start at the outer boundary if we approach the 2-phase region during unloading of Li, because in that case the Li fraction at r_0 will obviously be slightly smaller than in the interior.

4.2 Conservation of particle numbers

The total number N_{M} of $FePO_4$ units is conserved, and we can formulate its global conservation law $N_{\mathrm{M}} = N_{\mathrm{M}}^- + N_{\mathrm{M}}^+$, which reads more explicitly for the simplified case at

hand

$$\bar{n}_{\mathrm{M}}\bar{r}_0^3 = n_{\mathrm{M}}^- r_{\mathrm{I}}^3 + n_{\mathrm{M}}^+(r_0^3 - r_{\mathrm{I}}^3). \tag{4.1}$$

Recall that $\bar{n}_{\mathrm{M}}$ is the density of $FePO_4$ units in the deformation free reference state, i.e. $y = 0$ and $p = \bar{p}$. The outer radius of the host system in this state is denoted by $\bar{r}_0$.

The host system is an open system for Li, therefore the ratio q of the total number of Li atoms and the total number of interstitial lattice sites, i.e. $q(t) = N_{\mathrm{Li}}(t)/N_{\mathrm{M}}$, is a function of time and we have

$$q = \frac{n_{\mathrm{Li}}^- r_{\mathrm{I}}^3 + n_{\mathrm{Li}}^+(r_0^3 - r_{\mathrm{I}}^3)}{\bar{n}_{\mathrm{M}}\bar{r}_0^3}\ . \tag{4.2}$$

4.3 The mechanical problem

The mechanical problem which is formulated in Section 3.2 reads in radial coordinates

$$\begin{aligned} &\frac{\partial p}{\partial r} = 0 \quad \text{for} \quad r \in \Omega_{+/-}(t) \quad \text{and} \\ &p^- - p^+ = \frac{2\gamma}{r_{\mathrm{I}}} \quad \text{for} \quad r = r_{\mathrm{I}}(t). \end{aligned} \tag{4.3}$$

From $(4.3)_1$ we conclude

$$\begin{aligned} &p = p^+(t) \quad \text{for} \quad r \in \Omega_+(t) \quad \text{and} \\ &p = p^-(t) \quad \text{for} \quad r \in \Omega_-(t). \end{aligned} \tag{4.4}$$

We consider the case of fixed outer pressure p_0 and we use the boundary condition $p^+ = p_0$. Here the outer radius r_0 changes with time and must be calculated from the conservation law (4.1).

We insert the constitutive law (3.27) into $p^+ = p_0$ and into the interfacial condition

$(4.3)_2$ to obtain

$$\begin{aligned} n_{\mathrm{M}}^{+} &= \bar{n}_{\mathrm{M}}\Big(h(y^{+}) + \frac{1}{K}(p_0 - \bar{p})\Big) \qquad \text{and} \\ n_{\mathrm{M}}^{-} &= \bar{n}_{\mathrm{M}}\Big(h(y^{-}) + \frac{1}{K}\big(p_0 - \bar{p} + \frac{2\gamma}{r_{\mathrm{I}}}\big)\Big). \end{aligned} \tag{4.5}$$

Finally we solve the conservation law (4.1) for $r_0(t)$,

$$r_0^3 = \frac{1}{n_{\mathrm{M}}^{+}}\Big(\bar{n}_{\mathrm{M}}\bar{r}_0^3 + (n_{\mathrm{M}}^{+} - n_{\mathrm{M}}^{-})r_{\mathrm{I}}^3\Big). \tag{4.6}$$

Thus we are able to eliminate n_{M}^{+} and n_{M}^{-} in the chemical potentials, see (3.32) and (3.33), and we end up with chemical potentials that depend on the Li fractions y^{-}, y^{+} and on the interfacial radius r_{I}. Note that the possibility to treat the mechanical problem independent of the diffusion problem is an extraordinary case, which is meet here because we have ignored deviatoric stresses, so that the stress tensor reduces to a pressure. In the general case diffusion and mechanics must be solved simultaneously.

4.4 Evolution equations

Finally we exploit the evolution equations (3.26) for spherical symmetry. Recall, that we consider a regime where the particle densities are homogeneous in each phase. Then by integrating (3.4) over the inner core with radius r_I we get $v_{\mathrm{Li,M}}^{-}(t, r_{\mathrm{I}}) = r_{\mathrm{I}}\dot{n}_{\mathrm{Li,M}}^{-}/(3n_{\mathrm{Li,M}}^{-})$. We insert this result and $w^{\nu} = \dot{r}_{\mathrm{I}}$ in the definitions (3.7) and obtain

$$\dot{\mathcal{N}}_{\mathrm{Li}}^{-} = \frac{1}{3r_{\mathrm{I}}^2}\frac{d}{dt}\Big(n_{\mathrm{M}}^{-}y^{-}r_{\mathrm{I}}^3\Big) \qquad \text{and} \qquad \dot{\mathcal{N}}_{\mathrm{M}}^{-} = \frac{1}{3r_{\mathrm{I}}^2}\frac{d}{dt}\Big(n_{\mathrm{M}}^{-}r_{\mathrm{I}}^3\Big). \tag{4.7}$$

We use these identities in the left hand sides of the kinetic relations (3.26) and obtain

$$\frac{r_{\mathrm{I}}}{3}\frac{d}{dt}(n_{\mathrm{M}}^{-}y^{-}) + n_{\mathrm{M}}^{-}y^{-}\frac{dr_{\mathrm{I}}}{dt} = M_{\mathrm{Li}}^{\mathrm{I}}[[\mu_{\mathrm{Li}} - \mu_{\mathrm{V}} + \frac{m_{\mathrm{Li}}}{2}(v - w)^2]], \tag{4.8}$$

$$\frac{r_{\mathrm{I}}}{3}\frac{dn_{\mathrm{M}}^{-}}{dt} + n_{\mathrm{M}}^{-}\frac{dr_{\mathrm{I}}}{dt} = M_{\mathrm{M}}^{\mathrm{I}}[[\mu_{\mathrm{V}} + \frac{m_{\mathrm{M}}}{2}(v - w)^2]]. \tag{4.9}$$

These equations and the conditions (4.1), (4.2) determine the evolution of the interface radius $r_{\rm I}$ and of the atomic Li fractions $y^{+/-}$. To this end, however, one has to eliminate $n_{\rm M}^{+/-}$ by means of (4.5).

4.5 Dimensionless quantities

We introduce dimensionless quantities by means of the time scale of a typical charging/discharging experiment, t_0, and the radius $\bar{r}_0$ of the host system for $y = 0$,

$$\tau \equiv \frac{t}{t_0}, \quad \xi_{\rm I} \equiv \frac{r_{\rm I}}{\bar{r}_0}, \quad \xi_0 \equiv \frac{r_0}{\bar{r}_0}. \tag{4.10}$$

The dimensionless internal time scales are defined by

$$\tau_{\rm Li} = \frac{\bar{n}_{\rm M}\bar{r}_0}{M^{\rm I}_{\rm Li}\Omega t_0} \quad \text{and} \quad \tau_{\rm M} = \frac{\bar{n}_{\rm M}\bar{r}_0}{M^{\rm I}_{\rm M}\Omega t_0}\ . \tag{4.11}$$

Furthermore we define dimensionless versions of the density of the matrix lattice, the diffusion flux, chemical potentials, the surface tension, the bulk modulus, and the external pressure, viz.

$$\nu \equiv \frac{n_{\rm M}}{\bar{n}_{\rm M}}, \quad \tilde{\mu} \equiv \frac{\mu}{\Omega}, \quad \tilde{\gamma} \equiv \frac{\gamma}{\bar{p}\bar{r}_0}, \quad \tilde{K} \equiv \frac{K}{\bar{p}} \quad \text{and} \quad P \equiv \frac{p_0}{\bar{p}} - 1. \tag{4.12}$$

4.6 Summary of the model

In this section we give the explicit evolution system and initial and boundary data in dimensionless quantities for the two variables y^- and $\xi_{\rm I}$.

The evolution equations rely on the ODE system (4.8) and (4.9). The appearing kinetic energies are small for the case at hand and thus can be ignored. After some simple

rearrangements we have

$$\frac{1}{3}\nu^-\xi_{\rm I}\frac{dy^-}{d\tau} = \frac{1}{\tau_{\rm Li}}(\mu^+ - \mu^-) - y^-\frac{1}{\tau_{\rm M}}(\mu_{\rm V}^+ - \mu_{\rm V}^-), \tag{4.13}$$

$$\nu^-(\nu^- - \frac{1}{3}\frac{2\gamma}{K}\frac{1}{\xi_{\rm I}})\frac{d\xi_{\rm I}}{d\tau} = -\frac{h'(y^-)}{\tau_{\rm Li}}(\mu^+ - \mu^-) + (\nu^- + y^-h'(y^-))\frac{1}{\tau_{\rm M}}(\mu_{\rm V}^+ - \mu_{\rm V}^-)\ , \tag{4.14}$$

with $\mu^\pm := \mu_{\rm Li}^\pm - \mu_{\rm V}^\pm$. In favor of the readability we omit here the tilde over K, μ and γ. The conditions (4.1), (4.2) serve to determine y^+ according to

$$y^+ = \frac{q - y^-\nu^-\xi_{\rm I}^3}{1 - \nu^-\xi_{\rm I}^3}\ , \tag{4.15}$$

where $q(\tau)$ is the given total Li fraction.

The solution of the mechanical problem provides the dimensionless densities of the matrix particles in $\Omega_{+/-}$

$$\nu^+ = h(y^+) + \frac{P}{K} \quad \text{and} \quad \nu^- = h(y^-) + \frac{1}{K}\Big(P + \frac{2\gamma}{\xi_{\rm I}}\Big), \tag{4.16}$$

and the dimensionless external radius

$$\xi_0^3 = \frac{1}{\nu^+}\Big(1 + (\nu^+ - \nu^-)\xi_{\rm I}^3\Big)\ . \tag{4.17}$$

Finally we give the chemical potentials $\mu \equiv \mu_{\rm Li} - \mu_{\rm V}$ and $\mu_{\rm V}$ in terms of the dimensionless variables:

$$\mu = f'(y) - a_1\frac{h'(y)}{h(y)}\Big(1 - \frac{h(y)}{\nu}\Big) - a_2\frac{h'(y)}{h(y)^2}, \tag{4.18}$$

$$\begin{aligned}\mu_{\rm V} = {} & f(y) - yf'(y) + \\ & + a_1\left(\log\Big(\frac{\nu}{h(y)}\Big) + \frac{h'(y)}{h(y)}\Big(1 - \frac{h(y)}{\nu}\Big)y\right) \\ & + a_2\left(1 + \frac{h'(y)}{h(y)}y\right)\frac{1}{h(y)},\end{aligned} \tag{4.19}$$

The functions h and ν account for the mechanical contributions to the chemical potentials. Note that from (4.16) we have different representations for ν in $\Omega_{+/-}$, viz. $\nu^+(y^+)$

and $\nu^-(\xi_{\rm I}, y^-)$. Accordingly there result different functions that represent the chemical potentials in the two phases. For the case of fixed external pressure these are written as $\mu^+(y^+)$, $\mu^-(\xi_{\rm I}, y^+)$ and $\mu^+_{\rm V}(y^+)$, $\mu^-_{\rm V}(\xi_{\rm I}, y^-)$.

For given external pressure p_0 and given total Li fraction $q(\tau)$ one can by means of (4.15) and (4.16) write all variables in (4.13)-(4.19) as functions of y^- and $\xi_{\rm I}$. The system (4.13) - (4.19) is thus a closed system that will be used in the following to determine the evolution of the host system for various choices of initial data for $y^-(t_0)$, $\xi_{\rm I}(t_0)$.

5 Simulations

In this section we numerically study the proposed model (4.13) - (4.19). To this end we choose the following parameters as fixed:

The considered processes run at constant temperature $T_0 = 293.2$K and constant pressure $\bar{p} = p_0 = 1$bar, i.e. $P = 0$. The density of matrix particles is $\bar{n}_{\rm M} = 8.396\ 10^{28}$particles/m^3 (see [11]). The mechanical parameters bulk modulus, surface tension and maximal volume change are chosen as $K = 7.5\ 10^{10}$N/m^2 (see [12]) and $\delta = 0.06$ (deduced from [12]). We assume that $\gamma = 0.075$N/m. The free energy contains the interaction energy $\Omega = 94.4\ 10^{-22}$J/atom (see [11]) and the 3 parameters $a_0 = kT_0/\Omega = 0.390$, $a_1 = K/(\bar{n}_{\rm M}\Omega) = 11.5$ and $a_2 = \bar{p}/(\bar{n}_{\rm M}\Omega) = 0.000115$. Here $k = 1.38\ 10^{-23}$J/K denotes the Boltzmann constant. We choose the time scale of the model by $t_0 = 3h = 10800s$, this is a typical charging time of a battery and the length scale by $\bar{r}_0 = 20\ 10^{-9}$m.

The two relaxation times $\tau_{\rm Li}$ and $\tau_{\rm M}$ of the model are not known because they did not yet appear in the literature. However, we shall assume that they have values $\tau_{\rm Li} \leq 1$ and

$\tau_M \leq 1$. Thus we consider processes where the relaxation time of the interface is smaller or equal as the charging time t_0.

In Section 5.3 we will give a short discussion on the influence of the choices of τ_{Li} and τ_M to the evolution of the host system.

5.1 Chemical potentials

At first we discuss some properties of the chemical potentials $\mu \equiv \mu_{Li} - \mu_V$ and μ_V. Figures 4 and 5 show these two potentials without and with mechanical contributions. The mechanical phenomena are due to surface tension and Li induced volume changes of the matrix lattice. If these are ignored, i.e. $\delta = \gamma = 0$, we were to have $\mu = f'(y)$ and $\mu_V = f(y) - yf'(y)$ with f given by $(3.30)_2$. In this case the chemical potentials exclusively depend on the Li fraction y and any dependence on the radius ξ_I drops out.

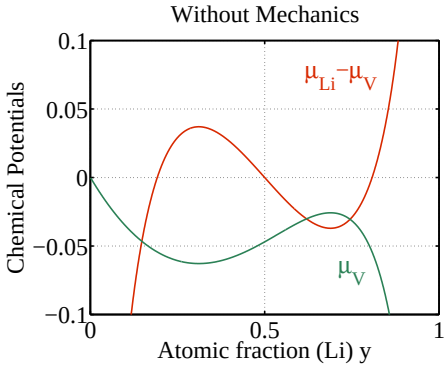

FIGURE 4. Relevant chemical potentials $\mu = \mu_{Li} - \mu_V$ and μ_V without mechanical contributions

If the mechanical phenomena are taken into account, the chemical potentials additionally depend on the location of the interface, i.e. on ξ_I. This dependence is illustrated in

Figure 5 by the blue and green curves, which give the chemical potentials μ and μ_{V} for two different locations of the interface, viz. $\xi_{\mathrm{I}} = 0.43$ and $\xi_{\mathrm{I}} = 0.10$.

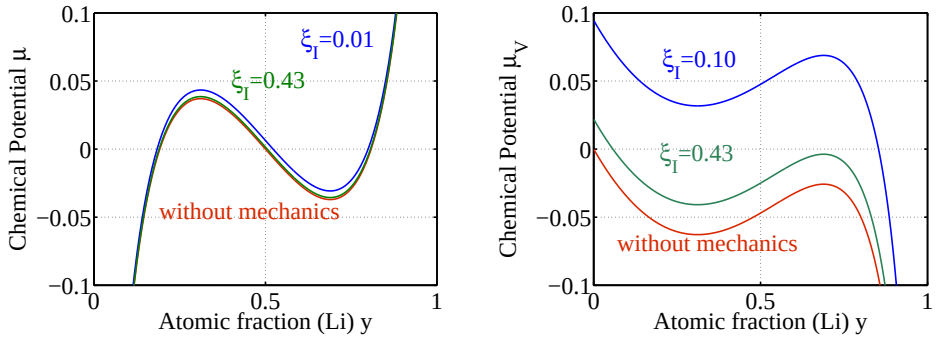

FIGURE 5. Red: Chemical Potentials as in Figure 4 without mechanical contributions. Blue and green: Chemical potentials with mechanical contributions for 2 different interfacial radii.

The difference $\mu = \mu_{\mathrm{Li}} - \mu_{\mathrm{V}}$ is hardly influenced by the location of the interface. This fact is important to understand the observed evolution of the voltage, which is determined by μ. On the other hand, the chemical potential of the vacancies μ_{V} depends quite sensitively on a variation of ξ_{I}. This fact is related to the origin of the hysteretic behavior of the charging/discharging process of the battery.

Finally we discuss the non-monotonicity of the chemical potentials. It is sufficient to consider the difference μ. Let the Li fractions $y_1 < y_2$ indicate the boundaries of the two regions $0 \leq y < y_1$ and $y_2 < y \leq 1$ where μ is uniquely invertible with respect to y. If the total Li fraction q lies in either one of those ranges the Li distribution of the host system is represented by a single phase. For $y_1 \leq q \leq y_2$, there are three Li fractions corresponding to a given value of μ and the host system may decompose into different phases which are separated by an interface. The explicit determination of the region

where the Li distribution is represented by two adjacent phases is a subtle problem that will be solved in the next sections of this study.

5.2 Possible equilibria

In this section we determine the possible equilibria for given total Li fraction $q \in (0,1)$.

The conditions for possible equilibria consists of the two equations (3.25), which guarantee zero interfacial entropy production,

$$\begin{aligned} \mu^+(y^+) &= \mu^-(\xi_{\mathrm{I}}, y^-) \quad \text{and} \\ \mu^+_{\mathrm{V}}(y^+) &= \mu^-_{\mathrm{V}}(\xi_{\mathrm{I}}, y^-), \end{aligned} \tag{5.1}$$

and of the Stefan condition (4.15)

$$y^+ = \frac{q - y^-\nu^-(\xi_{\mathrm{I}}, y^-)\xi_{\mathrm{I}}^3}{1 - \nu^-(\xi_{\mathrm{I}}, y^-)\xi_{\mathrm{I}}^3} \ . \tag{5.2}$$

At first it is instructive to ignore the mechanical contributions. In that case, according to (4.18) and (4.19), the equations (5.1) reduce to the classical common tangent construction

$$\begin{aligned} f'(y^+) &= f'(y^-) \qquad \text{and} \\ f(y^+) - y^+ f'(y^+) &= f(y^-) - y^- f'(y^-), \end{aligned} \tag{5.3}$$

which determine the so called Maxwell line. Up to a symmetry transformation the solution (y^+, y^-) of (5.3) is unique. The solution is indicated in Figure 6 by the two black dots. The symmetry of (5.3) implies that we may have $y^+ > y^-$ as well as $y^+ < y^-$. Furthermore it is important to note that a variation of the location of the interface does not change the equilibrium. After (5.3) is solved for (y^+, y^-) we may use the equation (5.2) in the form $q = (1 - \xi_{\mathrm{I}}^3)y^+ + \xi_{\mathrm{I}}^3 y^-$ to determine the interface radius ξ_{I}. Next we include the mechanical phenomena into the discussion of the system (5.1), (5.2). In that case the

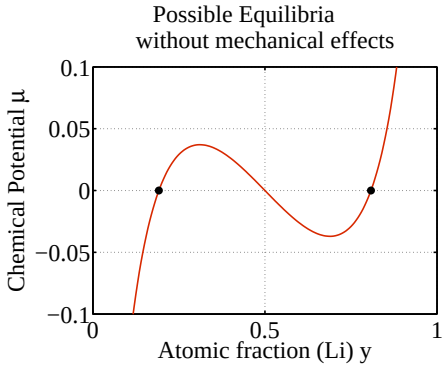

FIGURE 6. $\mu = \mu_{\mathrm{Li}} - \mu_{\mathrm{V}}$ and the two equilibria y^+ and y^- without mechanical contributions.

radius ξ_{I} of the interface appears in (5.1) and changes the solutions. This is shown in Figure 7 for various total Li mole fractions q. This should be compared with the simpler result in Figure 6 without mechanical effects. The solutions of the system (5.1) and (5.2) can be divided into two classes. One class consists of all solutions satisfying $y^+ > y^-$ (blue) and the other class is characterized by $y^+ < y^-$ (red). There is no symmetry anymore between these two cases.

The plot on the right hand side in Figure 7 gives the corresponding interfacial radii for given total Li mole fractions. It is important to note that there is a region (q_*, q^*), such that for given $q \in (q_*, q^*)$ two equilibria are possible.

5.3 On the origin of the hysteretic behavior

In this section we discuss the observed hysteretic behavior during a charging - discharging cycle, see Figure 2.

We assume that the experimentally observed hysteresis evolves via equilibria so that the data from the last section can be applied. For a comparison of our calculations to the behavior in Figure 2 we relate the quantities q and μ^+ to the capacity and the voltage

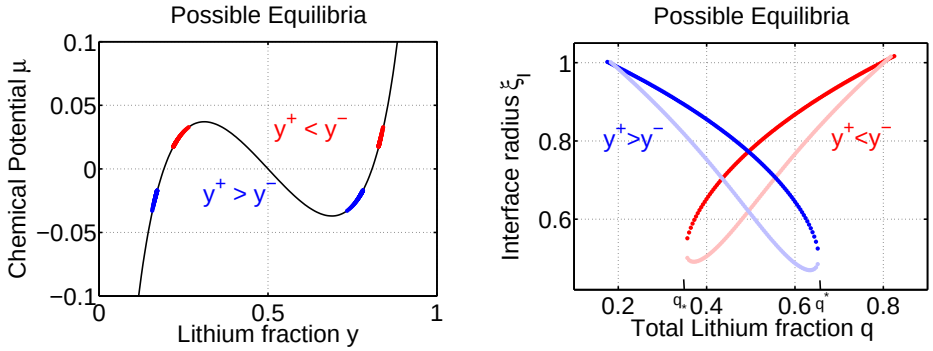

FIGURE 7. Possible equilibria when mechanical contributions are taken into account. Left: $\mu = \mu_{\mathrm{Li}} - \mu_{\mathrm{V}}$ and possible equilibria (y^+, y^-) for $y^+ > y^-$ (blue) and for $y^+ < y^-$ (red). Right : The corresponding interfacial radii ξ_{I} in equilibrium (dark colors). The points in light colors represent saddle points of the energy which also fulfill the necessary condition for equilibrium.

respectively. If the electrolyte is treated as a liquid with infinite conductivity and if the anode consists of metallic Li, it can be shown that the voltage U of the lithium cell is given by $U = -(\mu^+_{\mathrm{Li}} - \mu^+_{\mathrm{V}})/e + \mathrm{const.}$. The total charge capacity of the battery is related to the total amount of stored Lithium by $1 - q$.

We also need to decide which equilibria belong to charging and which belong to discharging respectively. We assume that in both cases the interface starts to appear at the outer radius. However, with $y^+ < y^-$ during charging and with $y^+ > y^-$ during discharging.

We now compare the calculated hysteresis plot of Figure 8 with the corresponding experimental data from Figure 2 and observe that the orientation of the two hysteresis loops are opposite to each other. This would indicate that one can extract energy in a charging-discharging cycle. Therefore it is likely, that the voltage-capacity behavior from Figure 8 has never been measured in any experiment.

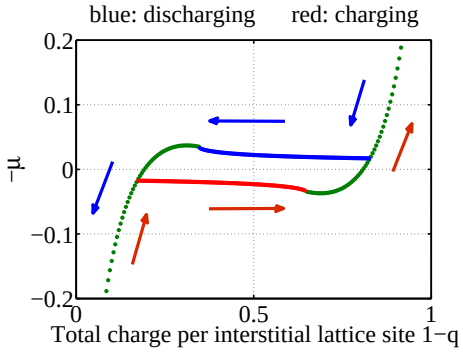

FIGURE 8. Equilibria states during charging and discharging. Regime of two coexisting phases: blue (discharging), red (charging). Single phase regime: green.

To resolve this paradox we take a closer look to the assembly of a lithium-ion battery. Typically a cathode consists of approximately 10^{10} to 10^{17} particles, see [5], which might not all behave the same. A model that deduces the battery characteristic from a single particle model thus might not be sufficient. This important observation forms the basis of a series of papers, [5, 2, 7], where the differences of a single particle model and a many particle model are discussed in detail.

However, even for a single particle electrode the described paradox is not acceptable. Therefore we proceed to make two crucial assumptions explicit that have lead to the hysteresis of Figure 8.

- Note that there are different branches in Figure 8, viz. those corresponding to two-phase equilibria and those that describe single-phase equilibria. Within the setting of a sharp-interface model, a priori, it is not evident how to connect these branches. In Figure 8 we considered the change from a single phase configuration to a double phase configuration to take place at $q = 0.17$ for discharging and at $q = 0.83$ for charging.

- We arbitrarily chose the surface tension to be $\gamma = 0.075$ N/m, because currently its proper value is not available.

A closer look to the free available energy concerning the nucleation points reveals, that the free available energy $\mathcal{A}_1$ is lower for a single phase configuration compared to $\mathcal{A}_2$ for a two phase configuration. In this context both energies are defined by

$$\mathcal{A}_1 = \int_\Omega \rho\psi dx + p_0 V \tag{5.4}$$

$$\mathcal{A}_2 = \int_{\Omega_-} \rho\psi dx + \int_{\partial\Omega_-} \sigma dx + \int_{\Omega_+} \rho\psi dx + p_0 V \tag{5.5}$$

with $\rho\psi$ from (3.18), V the particle Volume with $\Omega = \Omega_- \cup \Omega_+$, and p_0 is the constant outer pressure. Only within the region where the chemical potential μ has negative slope, the free available energy for a single phase configuration is larger than the two-phase energy. From this point of view a better choice is to assume that the switch from single phase to a two phase configuration occurs at the points of local extrema of μ, viz. $q = 0.31$ and $q = 0.69$.

Finally we substitute the surface tension $\gamma = 0.075$ N/m by $\gamma = 0.015$ N/m and obtain the charging/discharging behavior as is depicted in Figure 9. Thus the area enclosed by the graph in Figure 9 has now a positive sign and the paradox is resolved. Note that currently it is impossible to compare this curve with an experiment, since up to now we have no experiments with a single particle electrode. The interested reader may find further details of this important problem in [2, 5].

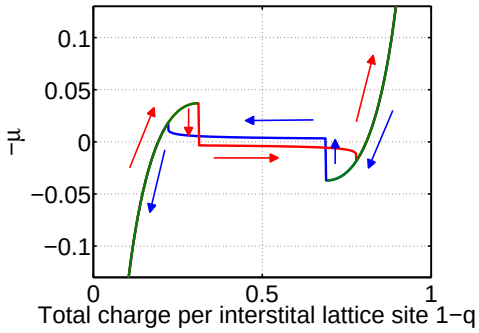

FIGURE 9. Possible charging/discharging cycle. Regime of two coexisting phases: blue (discharging), red (charging). Single phase regime: green.

5.4 Evolutions for various initial and boundary data

In this section we discuss the behavior of the ODE system (4.13)-(4.14) for various q. The basic variables are the Li fraction y^- in the inner region Ω_-, and the interface radius ξ_{I}. All other system properties depend on these two variables, or are given constants.

Here we consider a constant q, i.e. the total content of Li atoms in the storage system is constant during the evolution. In order to examine the evolutionary behavior of the ODE system (4.13)-(4.14) we examine the phase portrait. At first we discuss Figure 10, where

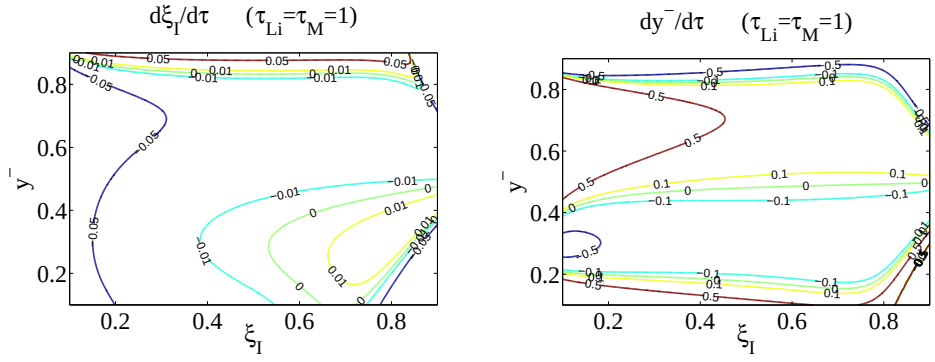

FIGURE 10. Visualization of phase portrait and domination of $\frac{\mathrm{d}y^-}{\mathrm{d}\tau}$

we study $\mathrm{d}\xi_I/\mathrm{d}\tau$ isolines (left) and $\mathrm{d}y^-/\mathrm{d}\tau$ isolines (right) for $q = 0.5$ and $\tau_{\mathrm{Li}} = \tau_{\mathrm{M}} = 1$.

We note that the change of the Li fraction is of one order higher than the interfacial speed $\mathrm{d}\xi_I/\mathrm{d}\tau$ so that at first the interfacial Li fraction settles to an equilibrium, i.e. this is a state where $\mathrm{d}y^-/\mathrm{d}\tau = 0$. Hereafter the system evolves possibly close to an isoline of $\mathrm{d}y^-/\mathrm{d}\tau = 0$ until the interface either reaches an equilibrium or it disappears, i.e. $\xi_I \to 0$ or resp. $\xi_I \to \xi_0$.

For the further discussion we write the ODE system (4.13)-(4.14) in a generic form and introduce the Jacobian J of the vector field F:

$$\begin{pmatrix} \mathrm{d}\xi_I/\mathrm{d}\tau \\ \\ \mathrm{d}y^-/\mathrm{d}\tau \end{pmatrix} = \begin{pmatrix} F_1(\xi_I, y^-) \\ \\ F_2(\xi_I, y^-) \end{pmatrix} \qquad \text{and}$$
$$J(\xi_I, y^-\tau) = \begin{pmatrix} \frac{\partial F_1}{\partial \xi_I} & \frac{\partial F_1}{\partial y^-} \\ \\ \frac{\partial F_2}{\partial \xi_I} & \frac{\partial F_2}{\partial y^-} \end{pmatrix} . \tag{5.6}$$

In this context an equilibrium is an asymptotically stable point of rest of the ODE. To this end it is necessary that the two isolines $\mathrm{d}\xi_I/\mathrm{d}\tau = 0$ and $\mathrm{d}y^-/\mathrm{d}\tau = 0$ must cross, see Figure 11(a). However such an intersection is in general only known to be a point of rest for the ODE but must not be asymptotically stable. Further stability analysis distinguishes an asymptotically stable point of rest from an unstable one. A necessary condition for a point of rest is $F(\xi_I, y^-) = 0$. If furthermore the eigenvalues of $J(\xi_I, y^-)$ have negative real parts, then this point of rest is asymptotically stable.

We proceed with the examination of Figure 11, which contains isolines $\mathrm{d}\xi_I/\mathrm{d}\tau = 0$ and $\mathrm{d}y^-/\mathrm{d}\tau = 0$. Due to the dominance of $\mathrm{d}y^-/\mathrm{d}\tau$ almost everywhere, the vector field F is only visualized at two selected points by a horizontal arrow pointing left or right for $sign(\mathrm{d}\xi_I/\mathrm{d}\tau) = \pm 1$, and a vertical arrow for $\mathrm{d}y^-/\mathrm{d}\tau$ respectively.

The directions of the arrows change their sign at the corresponding isolines $\mathrm{d}\xi_I/\mathrm{d}\tau =$

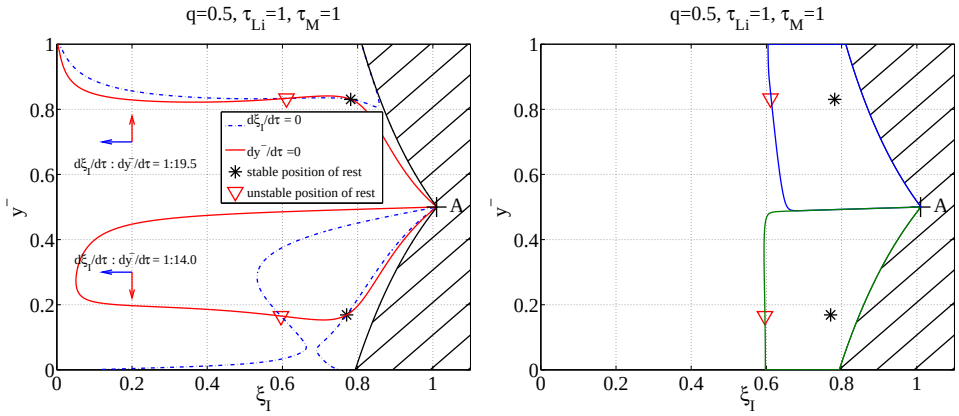

(a) isolines of zero horizontal or vertical flow (b) basin of attraction for positions of rest

FIGURE 11. Visualization of phase portrait

0 and $\mathrm{d}y^-/\mathrm{d}\tau = 0$, and thus one can reproduce the qualitative behavior of the field $F(\xi_I, y^-)$ in every point. In order to give an impression to the overall behavior of the system, we also indicate the ratio of the interface speed $\mathrm{d}\xi_I/\mathrm{d}\tau$ and the change of Li fraction $\mathrm{d}y^-/\mathrm{d}\tau$ at those two selected points.

We are interested in the area where $0 \leq y^+(y^-, \xi_I),\ y^- \leq 1$ and $0 \leq \xi_I \leq \xi_0(y^-, \xi_I)$. The non physical area is roughly shaded. A special point of interest is where the particle is single phase. Such a state can be realized by an inner radius of $\xi_I = 0$, $y^+ = q$ and y^- arbitrary. Furthermore there is the point A, depicted in Figure 11(a), which represents $\xi_\mathrm{I} = \xi_0$, $y^- = q$ and y^+ arbitrary. Recall that the ODE system at hand describes a two phase system and the set $S := \{(y^-, \xi_I) \in [0,1] \times 0\} \cup A$ embodies single phase states. Thus the ODE system is not defined on S and these states can only be considered in the sense of limiting states.

Inspecting the asymptotic behavior of the ODE system reveals, that taking an arbitrary point in the physical region as starting point for the ODE, only three different results can

occur in the asymptotical limit. The system ends either with a single phase ($\xi_I = 0$) or in one of the two stable points of rest, as depicted in Figure 11(a). To be precise, the system can theoretically also rest in asymptotically unstable point of rest. Such unstable point can even have an domain of attraction. However, since an arbitrary small disturbance of an unstable state drives the system into a stable point of rest or to a single phase state, we ignore this possibility.

The basins of attraction for the two asymptotically stable points of rest $(y_1^-(q), \xi_{I,1}(q))$ and $(y_2^-(q), \xi_{I,2}(q))$, are given in Figure 11(b). The whole region left of the two basins have the single phase with $\xi_I = 0$ as asymptotical limit. Each initial point in the vicinity of A, except A itself, lies in one of the basins of attraction.

This supports the assumption that phase separation in the particle starts at the outer boundary of the storage particle during loading or unloading.

Next we consider time dependent loading states $q(t) \in (q_*, q^*)$ with a small loading rate $\dot{q}$ on a time interval $t \in [t_0, t_1]$. Recall that in the region (q_*, q^*) two equilibria are possible. These are denoted by $(y_\ell^-(q(t)), \xi_{I,\ell}(q(t)))$ with $\ell = 1, 2$. We conclude from the ODE at hand, that a solution that starts closely to one of the equilibria $(y_1^-(q(t_0)), \xi_{I,1}(q(t_0)))$ at time t_0, stays within a small neighborhood of the time-dependent equilibrium $(y_1^-(q(t)), \xi_{I,1}(q(t)))$ for all $t \in [t_0, t_1]$. The same behavior is met for an initial value near the second equilibrium $(y_2^-(q(t)), \xi_{I,2}(q(t)))$. Thus if q remains within the two phase region, i.e. $q \in (q_*, q^*)$, the quasi-static model does not allow the transition from an inner core with high lithium fraction to an inner core with low fraction, or vice versa.

Next we discuss the case where one of the two possible equilibria disappears. To this

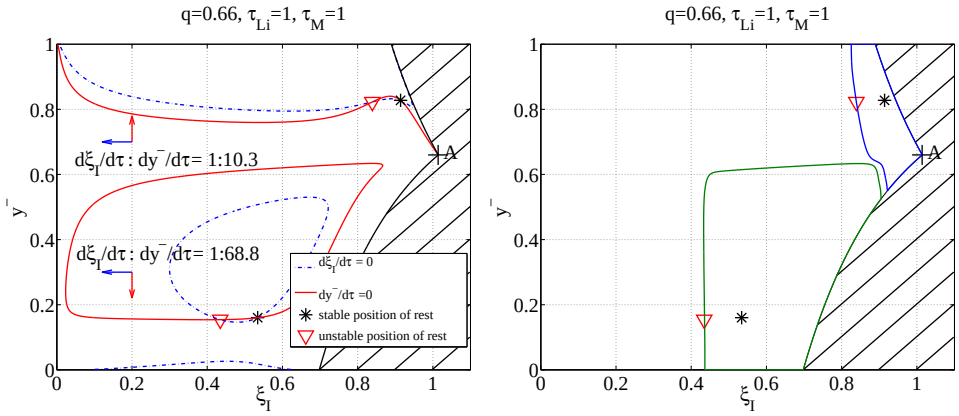

(a) isolines of zero horizontal or vertical flow (b) basin of attraction for positions of rest

FIGURE 12. Visualization of phase portrait for $\tau_{\mathrm{Li}} = \tau_{\mathrm{M}} = 1, q = 0.66$

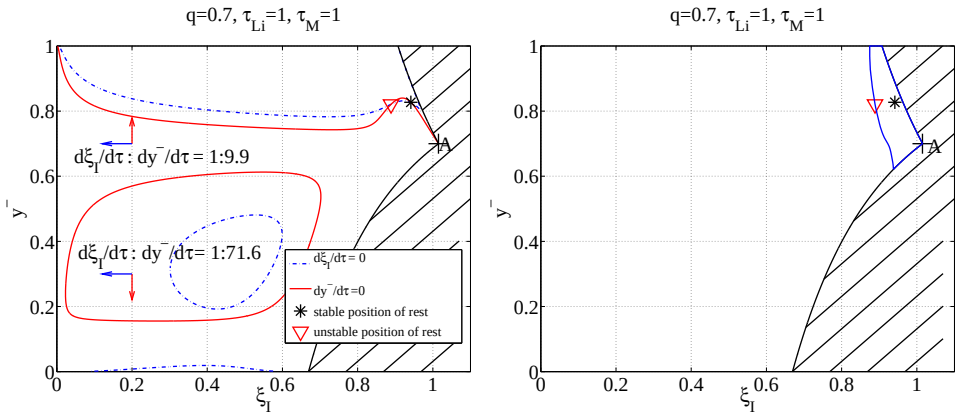

(a) isolines of zero horizontal or vertical flow (b) basin of attraction for positions of rest

FIGURE 13. Visualization of phase portrait for $\tau_{\mathrm{Li}} = \tau_{\mathrm{M}} = 1, q = 0.7$

end we study phase portraits for $q = 0.66$ and $q = 0.7$. These are given in Figures 12 and 13. There is a critical value q^* between 0.66 and 0.7, where the stable equilibrium with small mole fraction y^- disappears. We consider states in the area of attraction of that equilibrium. For $q > q^*$, these states belong to the area which has $\xi_{\mathrm{I}} = 0$ as its asymptotic limit, see Figure 13. Thus we conclude that a transition from an inner core

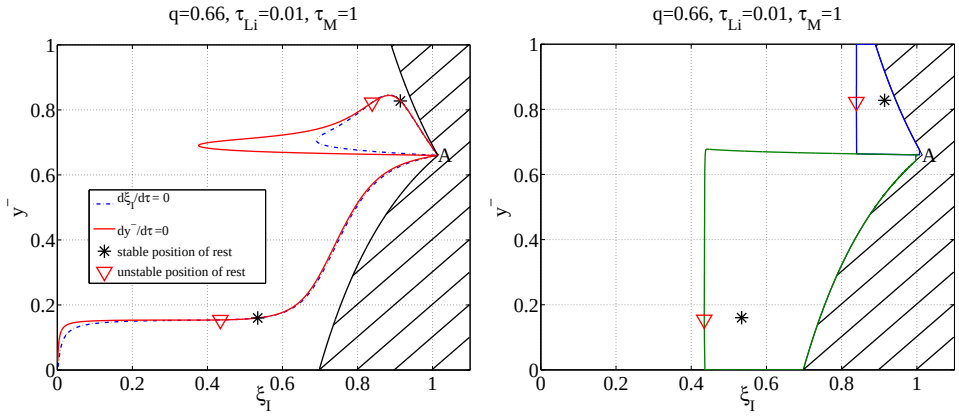

(a) isolines of zero horizontal or vertical flow (b) basin of attraction for positions of rest

FIGURE 14. Visualization of phase portrait for $\tau_{\mathrm{Li}} = 0.01, \tau_{\mathrm{M}} = 1, q = 0.66$

with low lithium fraction to an inner core with high lithium fraction at the critical value q^* is not possible. For q_* we meet the same behavior.

The Figures 12 and 14 show the effect of changing the mobilities τ_{Li} and τ_{M} on the basins of attractions. For $\tau_{\mathrm{Li}} = 0.01$ and $\tau_{\mathrm{M}} = 1$ we observe in contrast to to the former case $\tau_{\mathrm{Li}} = 1$ and $\tau_{\mathrm{M}} = 1$ that points close to the single phase state A can now reach both asymptotically stable points of rest. Note that independent of the choice of mobilities, the points of rest of the ODE (4.13)-(4.14) stay the same. Likewise, the stable state of an inner core with low lithium fraction also vanishes, as q increases over the same threshold value q^* as before, for other choices of the interface mobilities.

6 Conclusion

In this study we derive a model for a single $\mathrm{Li}_y\mathrm{FePO}_4$ particle that serves to store and release lithium in a lithium-ion battery. The resulting evolution equations describe

diffusion with mechanical coupling and incorporate volume changes of the $FePO_4$ crystal lattice, phase transitions and surface tension.

We study the equilibria of this model and discuss its behavior for quasi-static loading. The model justifies the assumption, that phase separation sets in at the outer boundary of the storage particle. In other words, a second phase is likely to be developed at the outer boundary in form of a growing outer shell.

For quasi-static loading the model implies that two different 2-phase configurations are possible as long as the loading state is between two thresholds $q \in (q_*, q^*)$. The stable 2-phase equilibria differ by high and low lithium fraction respectively, in the inner core.

The model does not allow to change from an inner core with high lithium fraction to an inner core with low fraction (or vice versa) in the two phase region $q \in (q_*, q^*)$. In other words: The single particle model implies that the battery voltage cannot change from one voltage plateau to the other if the loading state remains within the two-phase capacity regime.

However, in [5] we describe a crucial experiment where that transition between the voltage plateaus is observed for quasi-static loading. Thus we conclude that a model for a single particle cathode is not sufficient to describe the behavior of a common many particle battery. The statement is confirmed by a further phenomenon that is described in this paper: The single particle model yields an unexpected hysteresis loop compared to the experimental hysteresis. Nevertheless single particle models are still very popular in the chemical literature [11, 13, 14]. In [5, 6, 7] we develop a many particle storage system that is capable to predict the oberved hysteretic behavior in the voltage-capacity plot as well as transitions between the two voltage plateaus.

Acknowledgments

This work was performed as part of Project C26 "Storage of Hydrogen in Hydrides" of the DFG research center MATHEON, Berlin.

References

[1] Allen J.L., Jow T.R. and Wolfenstine J., Kinetic Study of the Electrochemical $FePO_4$ to $LiFePO_4$ Phase transition, Chemical Materials **19** (2004), 2108–2111.

[2] Delmas C., Maccario M., Croguennec L., Le Cras F. and Weill F., Lithium deintercalation in $LiFePO_4$ nanoparticles via a domino-cascade model, Nature materials, **7** (2008), pp. 665–671.

[3] Dreyer W., Jump conditions at phase boundaries for ordered and disordered phases, WIAS Preprint No. 869 (2003).

[4] Dreyer W. and Duderstadt F., On the modelling of semi-insulating GaAs including surface tension and bulk stresses, Proc. R. Soc. Lond. Ser. A Math. Phys. Eng. Sci., 464 (2008) pp. 2693-2720

[5] W. Dreyer, J. Jamnik, C. Guhlke, R. Huth, J. Moškon and M. Gaberšček, The thermodynamic origin of hysteresis in insertion batteries, Nature Materials **9** (2010), 448–453.

[6] Dreyer W., Guhlke C., Herrmann M., Hysteresis and Phase Transition in Many-particle Storage Systems, WIAS Preprint 1481 (2010), to appear in Continuum Mechanics and Thermodynamics

[7] Dreyer W., Guhlke C. and Huth R., The behavior of a many particle cathode in a lithium-ion battery, WIAS Preprint No. 1423 (2009), subbmitted to Physica D

[8] Gaberšček M., Dominko R. and Jamnik J., The meaning of impedance measurements of LiFePO4 cathodes: A linearity study, J. power sources **174** (2007), 944-948.

[9] Gaberšček M., Dominko R., Bele M., Remškar M., Hanzel D. and Jamnik J., Porous,

carbon-decorated LiFePO4 prepared by sol-gel method based on citric acid, Solid State Ionics **176** (2005), 1801–1805.

[10] Gomadam P.M. and Weidner J.W., Modeling Volume Changes in Porous Electrodes, Journal of The Electrochemical Society **153**(1) (2006), A179–A186.

[11] Han B.C., Van der Ven A., Morgan D. and Ceder G., Electrochemical modeling of intercalation processe with phase field models, Electrochimica Acta **49** (2004), 4691–4699.

[12] Maxisch T. and Ceder G., Elastic properties of olivine Li_xFePO_4 from first principles, Physical Review B**73** (2006), 174112-1–174112-4.

[13] Padhi A.K., Nanjundaswamy K.S. and Goodenough J.B., Phospho-olivines as Positive-Electrode Materials for Rechargeable Lithium Batteries, J. Electrochem. Soc. **144** (1997), 1188–1194.

[14] Srinivasan V. and Newman J., Discharge Model for the Lithium Iron-Phosphate Electrode, Journal of The Electrochemical Society **151**(10) (2004), A1517–A1529.

[15] Wagemaker M., Borghols W.J.H. and Mulder F.M., Large Impact of Particle Size on Insertion Reaction. A Case for Anatase Li_xTiO_2, J. AM. CHEM. SOC. **129**(14) (2007), 4323–4327.

[16] Yamada A., Koizumi H., Nishimura S.I., Sonoyama N., Kanno R., Yonemura M., Nakamura T. and Kobayashi Y., Room-temperature miscibility gap in Li_xFePO_4, Nature materials Letters **5** (2006), 357–360.